NASA
Contractor Report 195481

Army Research Laboratory
Contractor Report ARL–CR–231

Film Temperatures in the Presence of Cavitation

Harold G. Elrod
Columbia University
Old Saybrook, Connecticut

and

D. Vijayaraghavan
The University of Toledo
Toledo, Ohio

June 1995

Prepared for
Lewis Research Center
Under Contract NCC3–291

National Aeronautics and
Space Administration

U.S. ARMY
RESEARCH LABORATORY

FILM TEMPERATURES IN THE PRESENCE OF CAVITATION

Harold G. Elrod
Professor Emeritus Columbia University
14 Cromwell Court
Old Saybrook, CT 06475

D. Vijayaraghavan *
The Univ. Of Toledo
Toledo, Ohio 43606

* NASA Resident Research Associate at Lewis Research Center

1. INTRODUCTION:

The purpose of this note is to propose calculation procedures for temperature when portions of a lubricating film are cavitated. These procedures are suggested for use in conjunction with the treatment of temperature as presented in a recent paper [Elrod, 1991]. They are to be coupled with a cavitation algorithm [Elrod, 1981]. The proposed relations implement the Jakobsson-Floberg-Olsson cavitation model [See Dowson & Taylor, 1979]. That model considers the cavitated zone to be one of constant pressure, partially occupied by striations of liquid that extend rotationwise across the gap in Couette flow. Although known to have deficiencies, the JFO model represents a considerable improvement over earlier, more approximate models. Its accuracy will be tested to some extent by deviations in temperature found between experiment and the present analysis.

Figure 1 shows a cross-section of the central portion of a submerged, liquid-lubricated journal bearing. This particular configuration was chosen because it involves all aspects of the proposed analytical modelling, not because it is proposed for its practicality.

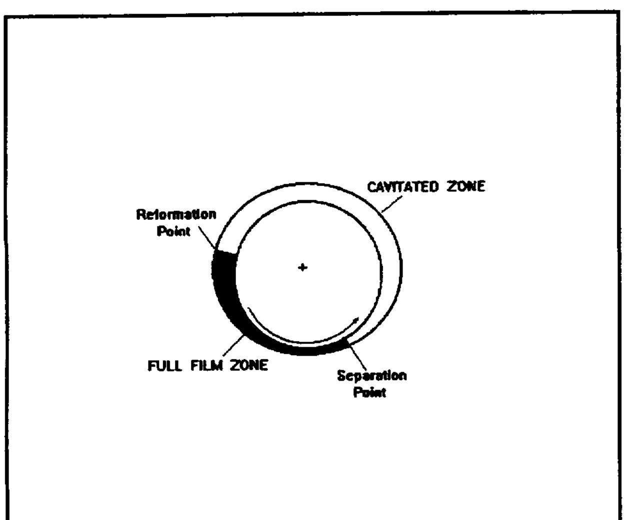

Figure 1 Schematic Diagram of Liquid-Lubricated Journal Bearing.

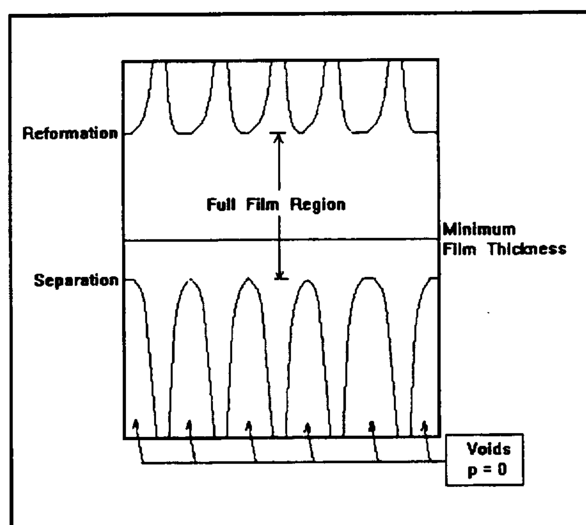

Figure 2 Stretched View of Lubricating Film Showing Cavitated and Full-Film Regions

There are two separate problems to be considered here. First, we have to choose an appropriate differential equation for the temperature within the cavitated zone. Second, we have to establish the inter-relations across the loci of separation and reformation.

2. THE TEMPERATURE EQUATION FOR THE CAVITATED ZONE:

JFO theory presumes that the liquid in the cavitated zone is completely in the form of striations (e.g. Figure 2). Accordingly, the temperature equation for this zone is the temperature equation for the striations. We begin by considering the relations for a single striation, and then generalize the results to a zone defined by separation and reformation loci.

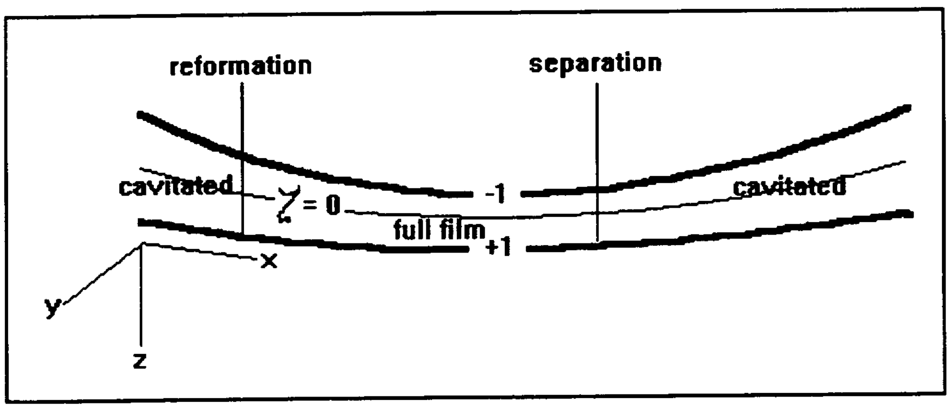

Figure 3 Coordinates Used in Analysis

Figure 3 defines the coordinates used in this analysis. The differential equation for the temperature of a full film is [Elrod, 1990, eq. 22]:

$$\partial T/\partial t + \underline{\underline{v}}\cdot\nabla T + (\partial T/\partial \varsigma) D\varsigma/Dt = (4/h^2)(\partial^2 T/\partial \varsigma^2) + \varphi/\rho C_p \qquad [2.01]$$

where:

$$D\varsigma/Dt = (-1/h)[(1+\varsigma)(\partial h/\partial t) + \nabla\cdot h\int_{-1}^{\varsigma} \underline{\underline{v}}\, d\varsigma] \qquad [2.02]$$

Here D/Dt is the Lagrangian time derivative, the vector $\underline{\underline{v}}$ is formed from the x and y components of the fluid velocity, h(x,t) is the film thickness, $\varsigma = 2z/h - 1$ and $\varphi = \mu[(\partial u/\partial z)^2 + (\partial v/\partial z)^2]$. The fluid density, ρ, and the specific heat, C_p, are taken as constant. The operator ∇ represents $\underline{\underline{e}}_x(\partial/\partial x) + \underline{\underline{e}}_y(\partial/\partial y)$, with both spatial derivatives taken at constant ς. Thus the last term in [2.02] can equally well be written as:

becomes[1]:

$$(\partial/\partial y)[\xi_p h^3(\partial p/\partial y)] = 12(\partial h/\partial t) + 6U(\partial/\partial x)[h(1 - \underline{\xi}_1/3\underline{\xi}_0)] \qquad [2.04]$$

Let us assume no transverse temperature variation, an assumption to be be verified a posteriori. Then:

$$\xi_p h^3(\partial^2 p/\partial y^2) = 12(\partial h/\partial t) + 6U(\partial h_c/\partial x) \qquad [2.05]$$

Now the striation is, itself, a segment of full film. We wish to evaluate $D\varsigma/Dt$ as determined by short-bearing theory. First we need $\partial v/\partial y$. The transverse momentum equation gives:

$$(\partial/\partial\varsigma)\mu(\partial v/\partial\varsigma) = (h/2)^2\partial p/\partial y \qquad [2.06]$$

The fluid viscosity, μ, is temperature dependent. Then with $\xi = 1/\mu$ we have:

$$\partial v/\partial\varsigma = (h/2)^2(\partial p/\partial y)\xi\varsigma + \beta\xi \qquad [2.07]$$

Or:

$$v = (h/2)^2(\partial p/\partial y)\int_{-1}^{\varsigma}\xi\varsigma d\varsigma + \beta\int_{-1}^{\varsigma}\xi d\varsigma \qquad [2.08]$$

At the upper plate the transverse velocity vanishes. Hence:

$$0 = (h/2)^2(\partial p/\partial y)\int_{-1}^{1}\xi\varsigma d\varsigma + \beta\int_{-1}^{1}\xi d\varsigma \qquad [2.09]$$

Therefore:

$$v = (h/2)^2(\partial p/\partial y)[\int_{-1}^{\varsigma}\xi\varsigma d\varsigma - (\underline{\xi}_1/3\underline{\xi}_0)\int_{-1}^{\varsigma}\xi d\varsigma] \qquad [2.10]$$

Take the y-derivative of eq. [2.10], neglecting, as before, the temperature variation in that direction. Now substitute for $\partial^2 p/\partial y^2$ its expression from [2.05]. We find:

$$(\partial/\partial y)(hv) = 3[\partial h/\partial t + (U/2)(\partial h_c/\partial x)]\xi_{int}/\xi_p \qquad [2.11]$$

where:

$$\xi_{int} = \int_{-1}^{\varsigma}\xi\varsigma d\varsigma - \underline{\xi}_1/3\underline{\xi}_0\int_{-1}^{\varsigma}\xi d\varsigma \qquad [2.12]$$

Note that if there is no transverse temperature variation within the striation, then there is no transverse variation of $\partial v/\partial y$.

For the shear-driven x-wise velocity component we have:

$$u = (U/2\underline{\xi}_0)\int_{-1}^{\varsigma}\xi d\varsigma \qquad [2.13]$$

---

[1] ξ_p is the mean fluidity for the local fluid layer, and is given by: $\xi_p = \underline{\xi}_0 + 0.4\underline{\xi}_2 - \underline{\xi}_1^2/3\underline{\xi}_0$. The $\underline{\xi}_i$ are the coefficients of an expansion for $\xi(\varsigma)$ in Legendre Polynomials.

$$v = (h/2)^2(\partial p/\partial y)\left[\int_{-1}^{\varsigma}\xi\varsigma d\varsigma - (\xi_1/3\xi_0)\int_{-1}^{\varsigma}\xi d\varsigma\right] \qquad [2.10]$$

Take the y-derivative of eq. [2.10], neglecting, as before, the temperature variation in that direction. Now substitute for $\partial^2 p/\partial y^2$ its expression from [2.05]. We find:

$$(\partial/\partial y)(hv) = 3[\partial h/\partial t + (U/2)(\partial h_c/\partial x)]\,\xi_{int}/\xi_p \qquad [2.11]$$

where:

$$\xi_{int} = \int_{-1}^{\varsigma}\xi\varsigma d\varsigma - \xi_1/3\xi_0\int_{-1}^{\varsigma}\xi d\varsigma \qquad [2.12]$$

Note that if there is no transverse temperature variation within the striation, then there is no transverse variation of $\partial v/\partial y$.

For the shear-driven x-wise velocity component we have:

$$u = (U/2\xi_0)\int_{-1}^{\varsigma}\xi d\varsigma \qquad [2.13]$$

From eqs. [2.11] and [2.13] we then obtain:

$$\nabla\bullet h\underline{\underline{v}} = (\partial/\partial x)(hu) + (\partial/\partial y)(hv) = (U/2)(\partial/\partial x)\left[(h/\xi_0)\int_{-1}^{\varsigma}\xi d\varsigma\right]$$

$$+ 3[\partial h/\partial t + (U/2)\partial h_c/\partial x](\xi_{int}/\xi_p) \qquad [2.14]$$

where $h_c = h(1 - \xi_1/3\xi_0)$.

To determine the indefinite integral of [2.14] we make us of the formula:

$$\int_{-1}^{\varsigma}\int_{-1}^{\acute{\upsilon}} f(\theta)\,d\theta d\acute{\upsilon} = \int_{-1}^{\varsigma}(1-\theta)f(\theta)\,d\theta \qquad [2.15]$$

We then obtain:

$$\nabla\bullet\int_{-1}^{\varsigma}h\underline{\underline{v}}d\varsigma = (U/2)(\partial/\partial x)(h/\xi_0)\left[\varsigma\int_{-1}^{\varsigma}\xi d\varsigma - \int_{-1}^{\varsigma}\varsigma\xi d\varsigma\right] +$$

$$3[\partial h/\partial t + (U/2)(\partial h_c/\partial x)]\int_{-1}^{\varsigma}(\varsigma-\theta)(\xi_{int}(\theta)/\xi_p)\,d\theta \qquad [2.16]$$

To check on this formulation, we carry out the designated integrations from -1 to +1. The result is:

$$\int_{-1}^{1}\nabla\bullet h\underline{\underline{v}}d\varsigma = -2(\partial h/\partial t) \qquad [2.17]$$

so that $D\varsigma/Dt$ from eq. [2.02] vanishes, as it should, at both the lower and upper film surfaces.

In the case of constant viscosity, eq. [2.16] becomes:

$$D\varsigma/Dt = [(1-\varsigma^2)/h][(\varsigma/2)(\partial h/\partial t) + U(\partial h/\partial x)(\varsigma+1)/4] \qquad [2.18]$$

Returning now to the differential equation [2.01] for temperature, we note that if $\partial T/\partial y = 0$, there are no terms in the equation to generate that component. Then identically the same differential equation applies across the striation width, and <u>the magnitude of the terms is independent of the striation width</u>. Although the above analysis was constructed for diminishing film thickness, this last fact encourages us to use the relations also for a <u>diverging film thickness</u>. The logic of such use lies in the facts that (a) films are known to support some tension and (b) rupture into a multiplicity of striations would not alter the applicable differential equation. We propose then to use [2.02] and [2.16] to trace the temperature throughout the cavitated zone, from locus of separation to locus of reformation.

3. <u>TREATMENT OF THE INTERFACES</u>:

We turn now to treatment of the interfaces between the cavitated and full-film zones. Figure 4 shows a small section of a reformation front. The flow in the cavitated zone is entirely in the x-direction. Matching flows normal to the front, we get:

$$\underline{\underline{m}}_{cav} \cdot \underline{\underline{n}} - \underline{\underline{m}}_{ful} \cdot \underline{\underline{n}} = V_n[\rho'_{ful} - \rho'_{cav}] \qquad [3.01]$$

Here $\underline{\underline{m}}$ is the lineal mass flow per unit time, ρ' is the film mass content per unit area and V_n is the front velocity normal to itself. For simplicity, we now write this relation for a constant-property fluid and <u>no motion</u> of the front.

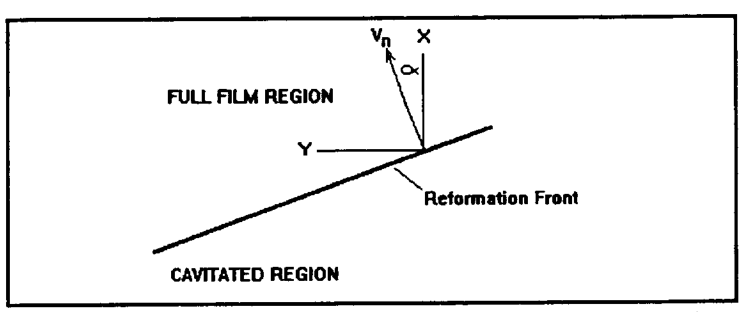

Figure 4. Schematic Diagram of Reformation Front

$$\cos(\alpha)\Theta\int_{-1}^{1}udz = \cos(\alpha)[Uh/2 - (h^3/12\mu)(\partial p/\partial x)] - \sin(\alpha)(h^3/12\mu)(\partial p/\partial y) \qquad [3.02]$$

Here Θ is the fractional liquid content on the cavitation side of the front.

Now the pressure is constant along the front. Therefore:

$$\cos(\alpha)(\partial p/\partial y) - \sin(\alpha)(\partial p/\partial x) = 0 \qquad [3.03]$$

Substitution of [3.03] in [3.02] gives:

$$\Theta U/2 = U/2 - (h^2/12\mu)(\partial p/\partial x)[1+\tan^2(\alpha)] \qquad [3.04]$$

To second order in angle α, mass continuity is expressed by the x-component of mass flux.

Figure 5 is a simplified cross-section of the streamlines in the neighborhood of the reformation front. On the cavitated side the flow is shear-driven until close to the front, at which location the striations rapidly spread transversely. On the full-film side there may be a region of reverse flow caused by the adverse pressure gradient. Complex though these phenomena may be, use of the cavitation algorithm has proved to give a satisfactory approximation. However, to treat the temperatures, as contrasted with the mass flows, a more detailed analysis must be attempted.

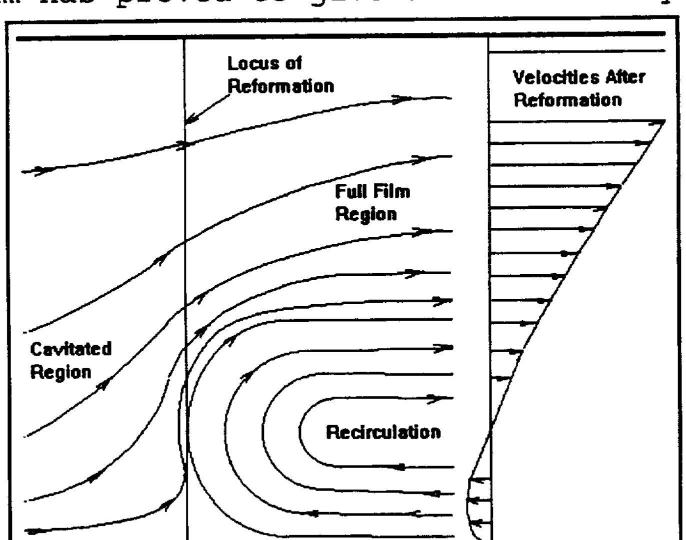

Figure 5. Diagram of the Streamlines Near Reformation Locus

In Figure 5 we show the flow from the cavitated region passing <u>over</u> the recirculating flow on the downstream side of the front. It is reasonable to suppose that over the small distances involved that the temperature associated with a fluid particle will not change much. Thus across the front we hypothesize that:

$$T = T(Q) \qquad [3.05]$$

where:

$$Q(\varsigma) = \Theta\int_{-1}^{\varsigma} u\,d\varsigma \text{ in the cavitated zone and} \qquad [3.06]$$

$$Q(\varsigma) = \int_{-1}^{1} u\,d\varsigma \text{ in the full-film zone.} \qquad [3.07]$$

Let us turn now to the recirculation zone. The velocities as shown in Fig. 5 are not precisely correct, for Reynolds Equation, as an asymptotic representation of Stokes Equation, does not yield the normal velocities, w, that would correspond to the bends in the depicted streamlines. Nevertheless, on the basis of the velocity distribution shown, we invoke again Eq. [3.05]. Progression upwards from the wall at $\varsigma=-1$ yields negative values of Q. The maximum negative value of Q is reached where u=0. Beyond this value, the Q's repeat until they finally become positive. We write:

$$\text{If } Q<0 \text{ then } T(Q, u>0) = T(Q,u<0) \qquad [3.08]$$

The point where the x-wise velocity, u, becomes zero is found from the following expression for velocity, taken from Elrod, 1990. Thus:

$$u = [U-(2\xi_1/3)B_x]\int_{-1}^{\varsigma}\xi d\varsigma/(2\xi_0) + B_x\int_{-1}^{\varsigma}\xi\varsigma d\varsigma \qquad [3.09]$$

where $B_x = (h/2)^2(\partial p/\partial x)$. And this velocity component vanishes when

$$[\int_{-1}^{\varsigma}\xi\varsigma d\varsigma/\int_{-1}^{\varsigma}\xi d\varsigma - \xi_1/(3\xi_0)][(h/2)^2 2\xi_0(\partial p/\partial x) = -U \qquad [3.10]$$

In the case of a constant-viscosity liquid, this last expression reduces to:

$$[(h/2)^2(\partial p/\partial x)/\mu U](1-\varsigma) = 1 \qquad [3.11]$$

In order for this equation to have a solution it is necessary for

$$(h/2)^2(\partial p/\partial x)/\mu U > 1/2 \qquad [3.12]$$

4. NUMERICAL EXAMPLES:

The foregoing analysis has been implemented numerically. As an example involving all aspects considered, we treat a bearing with the following geometry and lubricant characteristics.

Diameter = 0.25m; Length .2m

h_{mean} = .0001875m; Eccentricity = 0.85

Viscosity = .03 Ns/m^2; Thermal Diffusivity = 8E-8 m^2/s

Volumetric Specific Heat = 1.75E6 J/(m^3 °C)

Surface velocity = 39.27 m/s

All surface temperatures = 50 °C

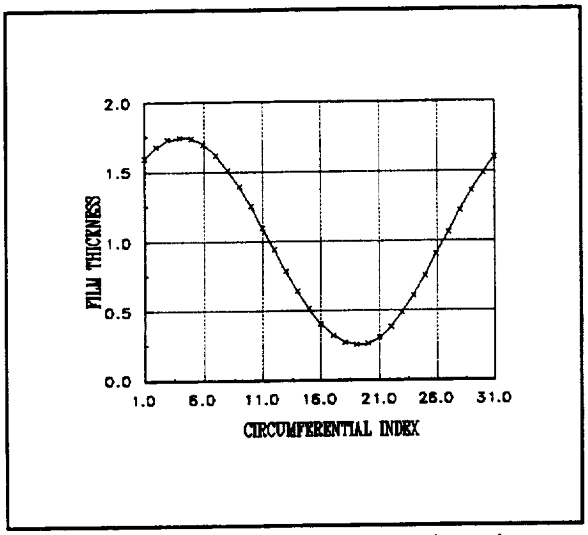

Figure 6. Film Thickness Distribution for Bearing Computations

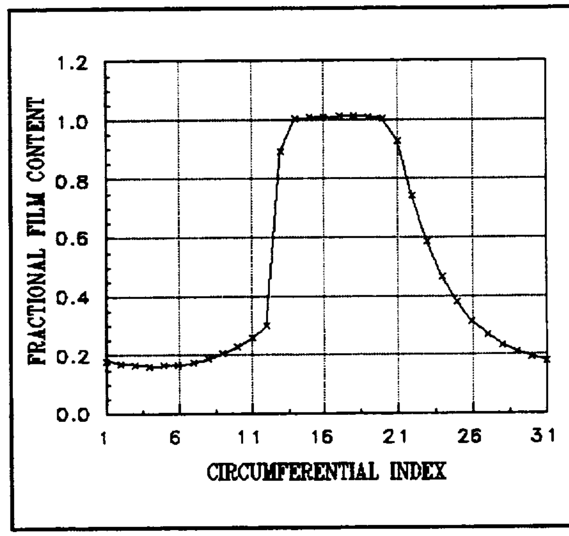

Figure 7. Fractional Film Content for Example Bearing

In the computations, the periphery was divided into 30 even increments. Figure 6 shows the chosen film thickness distribution. Figure 7 shows the fractional film content obtained with the viscosity held constant at the listed value. Under the circumstances, the film content and velocity distributions are independent of the liquid temperature. Figure 8 shows the velocity distributions just before and after reformation. As can be seen from Fig. 8, the index 13 is for the position immediately before reformation, whereas 14 and 15 lie just after. Note that station 14 shows some reverse flow in the region $-1<\varsigma<.5$ The backward flow in this region must return in a layer of positive velocity located adjacent to $\varsigma=0.5$. In the case of constant liquid viscosity, these velocity profiles, as well as the fractional mass content, are independent of the number of internal Lobatto points, so long as that number is greater than or equal to 2.

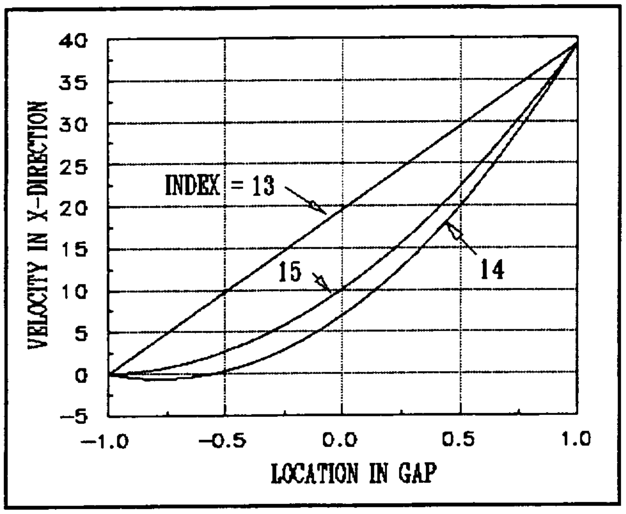

Figure 8. Velocity Distributions in Neighborhood of Reformation

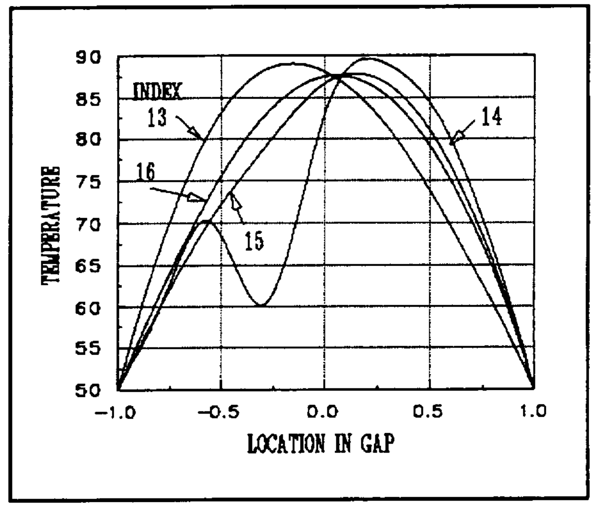

Figure 9. Temperature Profiles in the Neighborhood of Reformation

Figure 9 shows the temperature profiles on the bearing centerplane in the neighborhood of reformation for the case of 9 internal Lobatto points. Note the temperature reversal as ς proceeds from the lower wall. This reversal is in line with the streamline formation schematically shown in Fig. 5. For less numbers of Lobatto points this behavior is represented with less and less fidelity. For three Lobatto points it is shown not at all. Nevertheless, for this case in some average sense the features are preserved, for at station 15 (Figure 10) there is little difference in the resulting temperature distributions from 3 and 9 points.

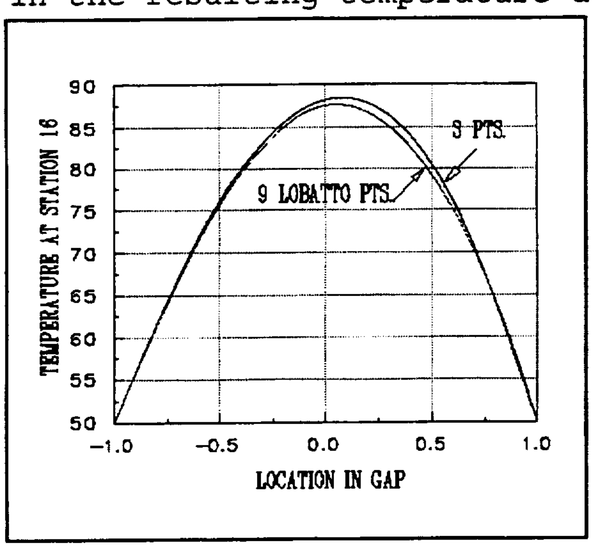

Figure 10. Comparison of Temperature Profiles at Station 15 for 3 and 9 Internal Lobatto Points

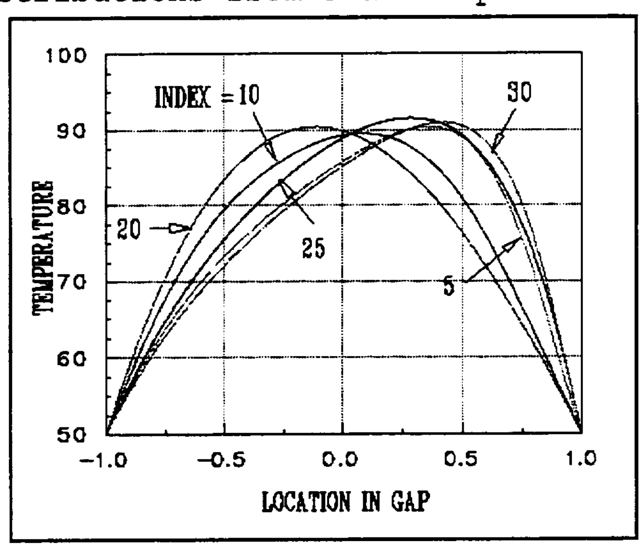

Figure 11. Shifting Temperature Profiles within the Striations

In Figure 11 we observe the shifting temperature patterns within the striations of the cavitated region. For steady-state operation and constant-viscosity lubricant, we have from eq. [2.18]

$$D\zeta/Dt = U(\partial h/\partial x)(1+\zeta)(1-\zeta^2)/4h$$

Hence if the film-thickness is increasing, the fluid tends to towards the upper plate, and vice versa. In the absence of film convergence or divergence, the temperature profile is symmetric between the walls, peaking at the middle.

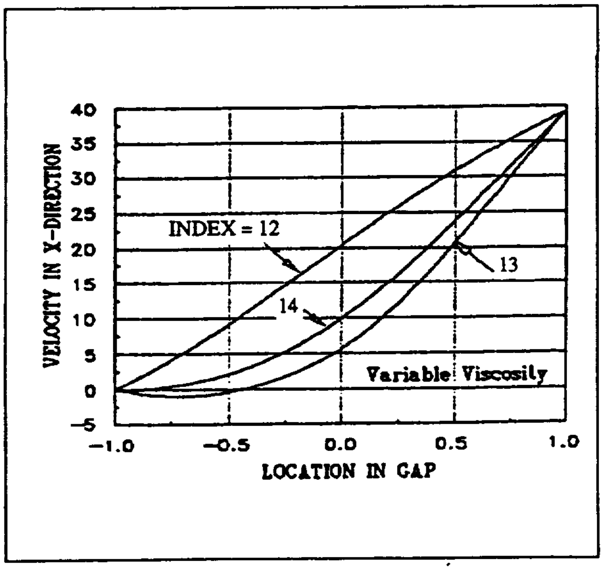

Figure 12 Velocity Distributions with Variable Viscosity

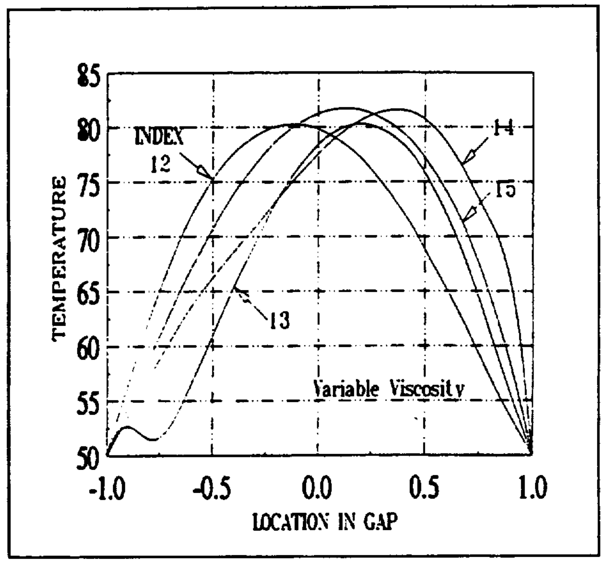

Figure 13. Temperature Profiles in Neighborhood of Reformation with Variable Viscosity

Figures 12-15 show some results obtained with the fluid viscosity varying according to the formula:

$$\mu = 0.03 \exp\{-0.01448(T-50°C)\} \text{ Ns/m}^2$$

The fluid viscosity diminishes with temperature, causing less overall temperature rise (See Figs. 13, 14 and 15). The velocity gradient midfilm is greatest because there the viscosity is least See Fig. 12). The reformation takes place slightly earlier (at index 13, instead of 14). Again downstream there is little difference between the results for 3 and 9 internal Lobatto points (See Fig. 14).

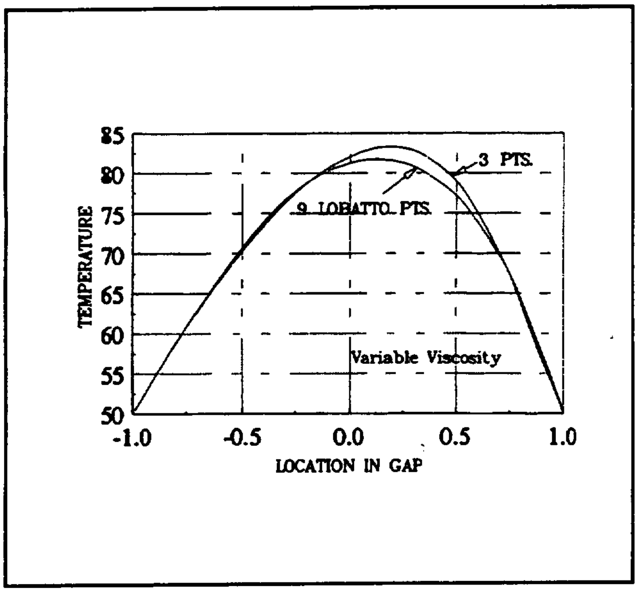

Figure 14 Temperature Profiles at Station 15 for 3 & 9 Internal Lobatto Pts., Variable Viscosity

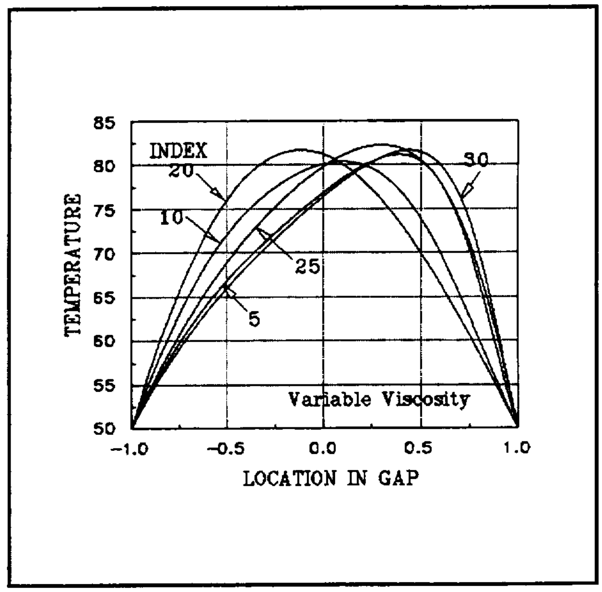

Figure 15 Shifting Temperature Profiles within the Striations

5. CONCLUSIONS:

Analysis and algorithms have been developed for the treatment of lubricating films involving cavitation and temperature effects. For purposes of illustration, the techniques have been applied to a simple, externally-flooded journal bearing. The work is considered to be a consistent extension of Jakobsson-Floberg-Olsson cavitation theory. Deviations between the present analysis and experiment may therefore lead to a better assessment of the validity of JFO theory[2]. Furthermore, the results presented here can be used as test cases for comparison by other investigators with other programs.

6. ACKNOWLEDGMENT:

It is a pleasure to acknowledge the assistance of David E. Brewe, Propulsion Directorate, U. S. Army Aviation Research and Technology Activity-AVSCOM, who monitored this investigation.

---

[2] For example, it is anticipated that the temperatures in the cavitation region will be over-estimated because JFO theory neglects the liquid that may be attached to one surface alone, and therefore not subjected to shearing.

7. NOMENCLATURE:

C_p	specific heat at constant pressure
h	film thickness
h_c	"convective" film thickness = $h(1-\underline{\xi}_1/3\underline{\xi}_0)$
p	pressure
Q	defined in eq. [3.06]
t	time
T	temperature
u	x-component of velocity
U	rotational velocity of shaft
v	y-component of velocity
$\underline{v}$	total velocity vector, $\underline{e}_x u + \underline{e}_y v + \underline{e}_z w$
$\underline{V}$	surface velocity vector. In this case, $\underline{e}_x U$
w	z-component of velocity
x	rotational direction coordinate
y	axial direction coordinate
z	direction normal to film, with value of 0 at half-way point
α	angle between the downstream-pointing normal to the reformation front and the unit vector in the x-direction
β	integration constant, eqs. [2.07] - [2.09]
ζ	dimensionless cross-film location, ranging from -1 to 1
θ	fractional liquid content of the film ϕ dissipation function, also dummy variable in eq. [2.15].
ϕ	$\mu[(\partial u/\partial z)^2 + (\partial v/\partial z)^2]$
μ	liquid viscosity
ξ	liquid fluidity, $1/\mu$
$\underline{\xi}_n$	coefficient of n^{th} Legendre polynomial in expansion for ξ
ξ_p	mean fluidity of film, defined in footnote of section 2.
ρ	liquid density

8. REFERENCES:

Elrod, H. G., 1991, "Efficient Numerical Method for Computation of the Thermodynamics of Laminar Lubricating Films," ASME Journal of Tribology, 113, 506-11.

Elrod, H. G., 1981, "A Cavitation Algorithm," H. G. Elrod, ASME Jnl. of Lub. Tech.,, 103, 350-4.

Dowson, D. & Taylor, C. M., 1979, "Cavitation in Bearings," Ann. Rev. Fluid Mechanics, 11, 35-66.

REPORT DOCUMENTATION PAGE

Form Approved
OMB No. 0704-0188

1. AGENCY USE ONLY (*Leave blank*)	2. REPORT DATE	3. REPORT TYPE AND DATES COVERED
	June 1995	Final Contractor Report

4. TITLE AND SUBTITLE
Film Temperatures in the Presence of Cavitation

5. FUNDING NUMBERS
WU–505–62–10
1L162211A47A
C–78749–C
NCC3–291

6. AUTHOR(S)
Harold G. Elrod and D. Vijayaraghavan

7. PERFORMING ORGANIZATION NAME(S) AND ADDRESS(ES)
Columbia University
14 Cromwell Court
Old Saybrook, Connecticut 06475

8. PERFORMING ORGANIZATION REPORT NUMBER
E–9713

9. SPONSORING/MONITORING AGENCY NAME(S) AND ADDRESS(ES)
Vehicle Propulsion Directorate
U.S. Army Research Laboratory
Cleveland, Ohio 44135–3191
and
NASA Lewis Research Center
Cleveland, Ohio 44135–3191

10. SPONSORING/MONITORING AGENCY REPORT NUMBER
NASA CR–195481
ARL–CR–231

11. SUPPLEMENTARY NOTES
Harold G. Elrod, Columbia University and D. Vijayaraghavan, The University of Toledo, Toledo, Ohio 43606 and NASA Resident Research Associate at Lewis Research Center (work funded under numbers C–78749–C and NCC3–291). Project manager, David E. Brewe, Materials Division, NASA Lewis Research Center, organization code 5140, (216) 433–6076.

12a. DISTRIBUTION/AVAILABILITY STATEMENT
Unclassified - Unlimited
Subject Category 34

This publication is available from the NASA Center for Aerospace Information, (301) 621–0390.

12b. DISTRIBUTION CODE

13. ABSTRACT ***(Maximum 200 words)***

In this note, numerical algorithms are developed and implemented for the treatment of laminar lubricating-film temperatures associated with cavitated regions. The reformation front, with its film-content discontinuity and flow reversal, is given special attention. Computational economy is achieved through the use of Lobatto-point locations for flow-property determinations.

14. SUBJECT TERMS
Fluid films; Thermal analysis; Liquid-vapor interfaces; Journal bearing; Hydrodynamics; Temperature distribution; Cavitation; Temperature Profiles; Bearings

15. NUMBER OF PAGES
15

16. PRICE CODE
A03

17. SECURITY CLASSIFICATION OF REPORT	18. SECURITY CLASSIFICATION OF THIS PAGE	19. SECURITY CLASSIFICATION OF ABSTRACT	20. LIMITATION OF ABSTRACT
Unclassified	Unclassified		